

AIDA-2020-CONF-2020-016

AIDA-2020

Advanced European Infrastructures for Detectors at Accelerators

Conference/Workshop Paper

Evaluating the Radiation Tolerance of a Robotic Finger

Marin-Reyes, H. (The University of Sheffield) *et al*

25 July 2018



The AIDA-2020 Advanced European Infrastructures for Detectors at Accelerators project has received funding from the European Union's Horizon 2020 Research and Innovation programme under Grant Agreement no. 654168.

This work is part of AIDA-2020 Work Package 15: **Upgrade of beam and irradiation test infrastructure.**

The electronic version of this AIDA-2020 Publication is available via the AIDA-2020 web site <http://aida2020.web.cern.ch> or on the CERN Document Server at the following URL: <http://cds.cern.ch/search?p=AIDA-2020-CONF-2020-016>

Copyright © CERN for the benefit of the AIDA-2020 Consortium

Evaluating the Radiation Tolerance of a Robotic Finger^{*} ^{**}

Richard French, Alice Cryer, Gabriel Kapellmann-Zafra, and Hector Marin-Reyes

The University of Sheffield, Western Bank, Sheffield, S10 2TN, UK
h.marin-reyes@sheffield.ac.uk

Abstract. In 2024, The Large Hadron Collider (LHC) at CERN will be upgraded to increase its luminosity by a factor of 10 (HL-LHC). The ATLAS inner detector (ITk) will be upgraded at the same time. It has suffered the most radiation damage, as it is the section closest to the beamline, and the particle collisions. Due to the risk of excessive radiation doses, human intervention to decommission the inner detector will be restricted. Robotic systems are being developed to carry out the decommissioning and limit radiation exposure to personnel. In this paper, we present a study of the radiation tolerance of a robotic finger assessed in the Birmingham Cyclotron facility. The finger was part of the Shadow Grasper from Shadow Robot Company, which uses a set of Maxon DC motors.

Keywords: Radiation, Robotic Grasping System, Radioactive Environment

1 Introduction

The Large Hadron Collider (LHC) at CERN in Geneva, Switzerland is the largest particle accelerator in the world. It collides high-energy hadrons to create subatomic particles, which are detected and studied by the 4 main experiments along the beamline. One of these is ATLAS, a large multipurpose detector which is formed of multiple sub-detectors, each devoted to particle identification and tracking [6]. In 2024, the LHC will be upgraded to increase its luminosity by a factor of 10 (HL-LHC). The ATLAS inner detector (ITk) will be upgraded at the same time. As it is the section closest to the beamline, and therefore the particle collisions, it has suffered the most radiation damage. The detector is anticipated to emit 1.1 mSv/h at 10 cm from the beamline at shutdown [9,11].

Robotic grasping systems and end effectors are an important element of a decommissioning robot. For the future decommissioning of the ATLAS inner

^{*} This project has been funded by Innovate-UK under their "Energy Game Changer" collaborative research and development programme.

^{**} This project has received funding from the European Union's Horizon 2020 Research and Innovation programme under Grant Agreement no. 654168

detector, a robotic manipulator composed of three complex fingers is required to have a certain amount of dexterity. This to prevent any type of damage to the outer detector components. A finger from a human-like robotic hand has been previously assessed for their radiation tolerance, and are an ongoing area of R&D for our industrial collaborator, the Shadow Robot Company [9,11]. In this paper we focus on a finger from their more robust and industrial-like robotic manipulator.

2 Related Work

Complementary Metal Oxide Semiconductor (CMOS) chips seem to have definitively overtaken CCDs in the semi-conductor industry. However scaling circuitry complexity and density leaves electronics increasingly susceptible to radiation damage. Total Ionizing Dose (TID) effects occur when incident radiation ionizes atoms in the target material. Electron-hole pairs are generated, either by the initial interaction, or by secondary particles. The build-up of these pairs at interfaces within the semiconductor layers changes the behaviour of the switches by increasing leakage current and the $1/f$ noise in a CMOS device[3]. The change in performance from a compromised CMOS has detrimental knock on effects in the rest of the circuitry. As the devices are scaled down, the layers susceptible to damage get thinner, exacerbating the problem[3].

Many different applications for robotic systems have been identified in the nuclear industry. Radiation hardened robotics has gained a lot of interest as robots involvement in radioactive environments are more complex to those in other industries [17]. Mainly because of legal and ethical limitations on radiation exposure, as a consequence, robotic systems are more in need to be deployed in radioactive environments [16,2].

Space instrumentation conducts an extensive amount of research into how radiation affects electronics, however the levels of radiation between the space and nuclear environments differ by orders of magnitude [16]. Multiple attempts to test robotic systems under radioactive conditions have been reported through literature. The Quince rescue robotic platform was tested under similar conditions to the Fukushima power plant [15]. Development and testing of a tele-operated underwater maintenance robot for inspecting reactor coolant demonstrated to work under 30 m of water, and accomplish small maintenance tasks such as would be expected inside a nuclear cooling system [12]. However, it was never tested while working with radioactive materials. A bridge transported servo-manipulator with individual motor modules which could be remotely repaired is proposed as a long term solution [10]. Even multi-robot systems have been proposed to help detect radiation sources [4]. Nevertheless, tests have always been performed over full systems instead of focusing on testing and perfecting particular modules and components.

On the other hand, when testing electronic systems, it is less common for entire circuit boards to be irradiated, instead concentrating on the characterization of sensors and other electronic 'weak spots'.

Decommissioning projects often use commercial-off-the-shelf (COTS) components. Without the need for bespoke parts, the costs are lower and enables the system to be easily repaired. Fail-safe components such as a voltage regulators have been explored. It was found that the degradation of micro-controllers in the environment was predictable [18]. Similar to electronics, the study and testing of hardware should be also focused on the 'weak spots' of a robotic system.

3 Experimental Setup

The irradiation facility in the Medical Physics Dept of the University of Birmingham uses a Scanditronix MC40 cyclotron to produce a beam of protons of energy up to 40 MeV. It was commissioned to create Krypton radio nuclides for UK hospitals. Now it is also used to evaluate radiation tolerance for detector components for the ATLAS detector upgrade, as well as for industry hardware [8,7,14]

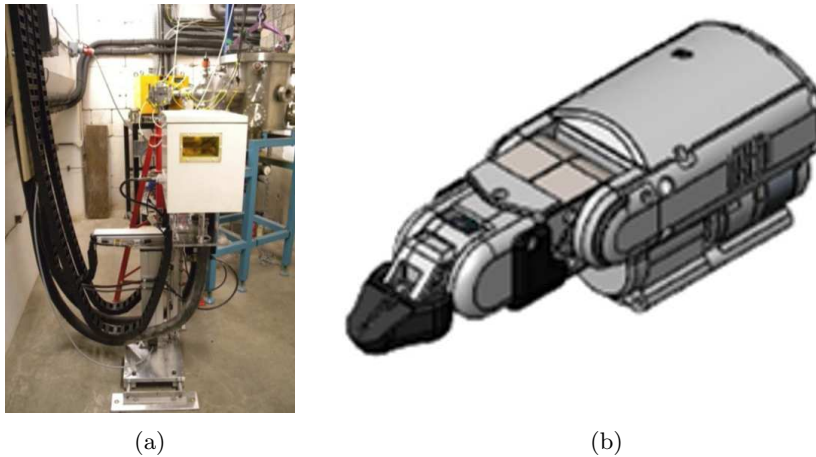


Fig. 1: a) The Birmingham cyclotron test box setup over a robotic scanner. b) CAD model of the Shadow Grasper finger.

The tested robotic finger was part of a robotic manipulator called the Shadow Smart Grasping System by the Shadow Robot Company. It is composed of three similar fingers and a base. It was placed inside a box located in the cyclotron beam (see Fig. 1a). It was programmed with a constant routine to keep it in motion. This to facilitate the detection of any faults during the irradiation. The routine involved the movement of two of three Maxon motors (see Fig. 3), and within this study the beam was targeted to only one specific motor (Maxon 18 V DC). The box had no cooling, as during the experiment a webcam was used

to observe the finger's movement routine (see Fig. 1b). The window where the beam enters the box is visible in Figures 2a and 2b. Gafchromic film was used to show where the beam had struck the finger.

The static proton beam area was of 1 cm^2 and its intensity has a penetration limit of 8 mm (measured with water). The stopping power and average density of the finger were calculated in order to calculate how long the finger would need in the beam.

The approximate stopping power of a compound material is calculated by summing the stopping power of the component materials multiplied by their fractional weight [13]. The values for the stopping power of the component materials were taken from the NIST database[5].

$$\left(-\frac{dE}{d\chi}\right)_{comp} = \sum_i w_i \left(-\frac{dE}{d\chi_i}\right)_i \quad (1)$$

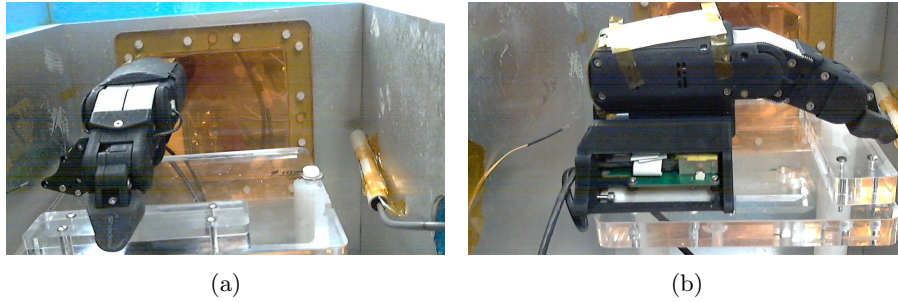


Fig. 2: Webcam images of the finger a) The first orientation, the finger applies pressure on the block below b) Second orientation showing gafchromic film, the finger applies pressure on block below.

Due to the thickness of the finger case creating a high resistance to the beam, two orientations of the finger were assessed. Figure 2a shows the orientation of the first irradiation and Figure 2b the second. During the first orientation (Fig. 3), the beam was directed through the length of the finger. This so that the finger movement would cause it to move in and out of the beam. The second orientation had the beam perpendicular to the base (Fig. 4).

The finger's routine was 15 seconds long and had to be continuous at all times to facilitate the detection of any fault. First the main body joint twists, followed by the curl of the phalanges' joint to form a hook (see Fig. 3b and 4b). The system then moves back to the original position following the same trajectory, where the fingertip applies pressure to a representative block of plastic directly underneath (see Fig. 3c and 4c). This was implemented to observe how the pressure sensor reacted in the radiated environment. After that, the finger relaxes the pressure on the block and commences the routine again.

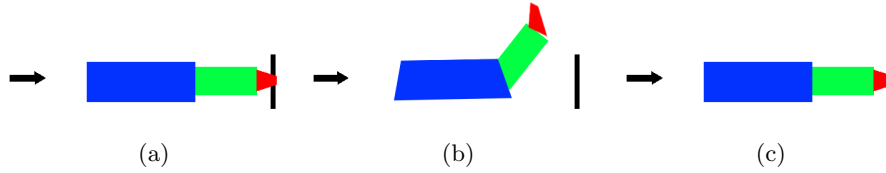


Fig. 3: a) The finger starting position. b) The finger rotates sideways and curls perpendicular to the beam. c) The finger uncurls and applies pressure to the block below.

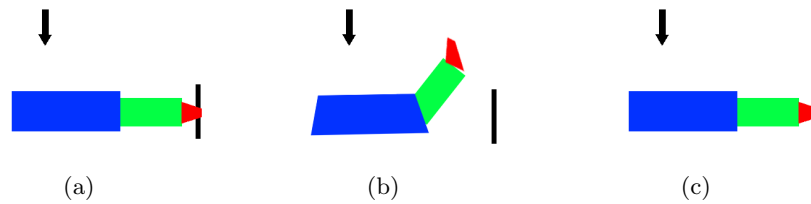


Fig. 4: a) The finger starting position. b) The finger rotates sideways and curls into the beam. c) Finger uncurls and applies pressure to the block below.

4 Results

For the first irradiation the finger was orientated as in Fig. 2a, it was irradiated with the beam set at 23 MeV protons at 10 nA. It spent two-thirds of the total irradiation time within the beam. Because the casing was 8 mm thick, some gafchromic film was placed between the casing and the interior to verify penetration of the beam. This irradiation lasted 18 minutes where the beam traced over an area of 7 cm x 1 cm. The localized area received a targeted total dose of 24.2 kGy with no apparent loss of casing integrity. The dose calculation was adjusted to reflect that the beam did not penetrate through the casing, which is PA12 Nylon. In total, the irradiated dose of the whole finger at this point is 727 Gy.

In the second irradiation the finger was orientated as in Fig. 2b, it was irradiated with the beam set at 23 MeV protons at 5 nA (this was due to a current drift of the cyclotron beam). It spent one third of the total radiation time in the beam. In this new orientation, the casing was 2 mm thick, and the beam remained static and was aimed directly at a finger motor driver. The finger stopped working after 9 minutes. It received 2.1 kGy at this 7 cm x 1 cm specific area irradiation. This was calculated using the stopping power for the whole finger. After this irradiation the TID of the finger was 91 Gy. At failure, the total irradiated dose of the entire device was 818 Gy.

This is significantly more than the radiation dose expected for the ATLAS decommissioning, which was estimated to be around 1 mSv/hour [9]. A human radiation worker's dosage is limited by the ICRP in 2007 to 50 mSv/year maxi-

mum, and 20 mSv average over 5 years. The weighting factor for protons is set at $W = 2$, so the robotic manipulator was irradiated with 1.6 kSv, orders of magnitude higher than acceptable human exposure[1].

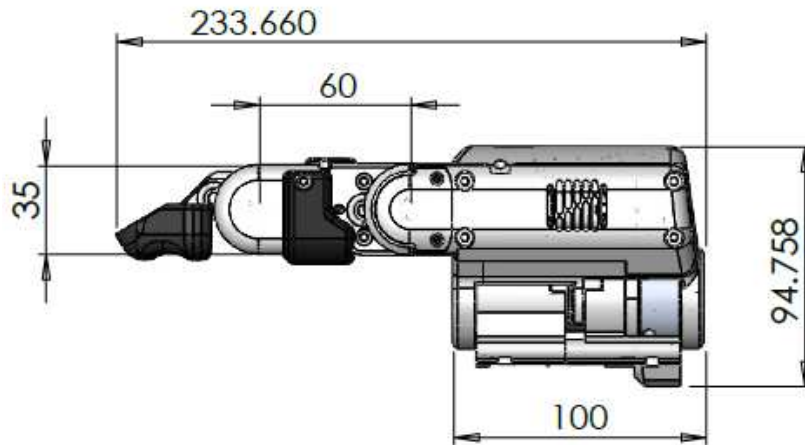


Fig. 5: Side view of the finger

Figure 5 shows a side view of the finger. The three segments are clearly visible. The base is 100 mm, and its joint rotates out of the page. The second segment is 60 mm long and the joint rotates on the plane of the page. The final segment is 73.66 mm, and the joint rotates on the plane of the page

Figure 6 presents the logged data from the finger's base motor and Fig. 7 presents the logged information of the finger's joint and tip. Except for Fig. 6a which presents the commands and target positions sent to all the fingers' motors, and Fig. 6b which presents the fingers' internal sensed temperature for each joint, the rest of the figures show a disruption at 9 minutes.

Figure 6b presents the temperature of the three motors through the 10 minutes of the second irradiation. It is evident that motor 1 (the base motor) was the one being irradiated. This graph shows a clear rise of the motors' temperature as time passes. We suspect that around minute 5, the sensing hardware or communication drivers were also affected, as the temperature readings change abruptly. The temperature sensors are analog based, this could mean that the ADC could have suffered some damage. However, we do not have enough evidence to declare what exactly affected the readings. This, of course, will be further investigated.

Figure 6c presents the measured position of the finger base motor and Fig. 6d presents the error measured between the current position and the desired targeted position. After 9 minutes it is possible to see that the sensor stopped detecting a change of position, and through webcam feedback we could see that the finger had stopped moving, most likely meaning that the chip driving the

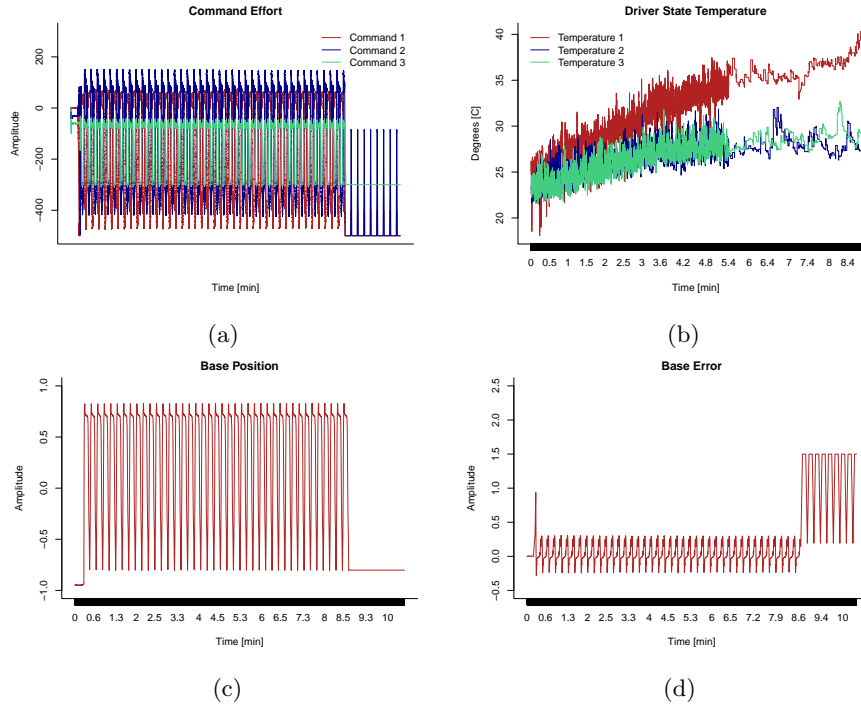


Fig. 6: a) Commanded target positions to all the motors. b) Internal sensed temperatures of the motors. c) Sensed position of the finger base motor. d) Error measured between the targeted position and the real position of the finger base motor.

motor had been damaged. As expected, the error became big when the motor stopped moving.

Figure 7a presents the measured position of the finger joint and Fig. 7b presents the error regarding the joints' position. Similarly, Fig. 7c presents the measured position of the fingertip and Fig. 7d presents its error. These graphs show a total stop of motion from the joint and tip motors. This happened due to the continuous routine constraint. The program was set to wait for the base motor to reach to a certain position before moving the other sections of the finger. Because the base motor had failed and was no longer moving, the other motors could not start their programmed motion.

5 Conclusion

After a total irradiated dose of 818 Gy to the entire device, the Shadow Grasper manipulator proved to be significantly resistant to radiation, and would be suitable for use in radioactive environments. A sample area of casing was irradiated

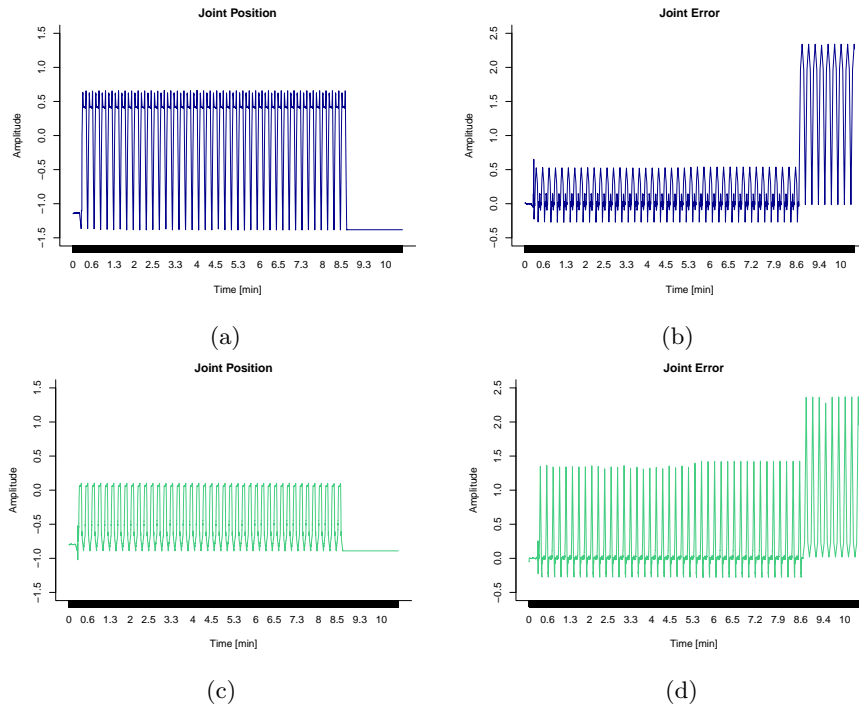


Fig. 7: a) Sensed position of the finger joint motor. b) Error measured between the targeted position and the real position of the finger joint motor. c) Sensed position of the finger tip motor. d) Error measured between the targeted position and the real position of the finger tip motor.

to 24.2 kGy with no apparent loss in integrity. A second irradiation experiment within the cyclotron vault has been proposed. Further tests are needed to detect weak areas of the electronic design, and to assess the manipulator's resistance to a broader range of radiation. As well, working routines need to be better designed to prevent the system from blocking itself.

Acknowledgments

We are very grateful to Shadow Robot Company, especially Annagiulia Moracholi, Gavin Cassidy and James Southall-Andrews for their invaluable support. We also thank the University of Birmingham, especially Tony Price, Laura Gonella and Philip Allport for setting up the proton beam and for their help in installing our apparatus.

References

1. The 2007 recommendations of the international commission on radiological protection. icrp publication 103. *Annals of the ICRP* 37(2-4) (2007)
2. Alexandre, J.M.: Electronic system operating under irradiation, process for designing such a system and application thereof to the control of a mobile robot (Nov 2 2004), uS Patent 6,812,476
3. Barnaby, H.: Total-ionizing-dose effects in modern cmos technologies. *IEEE Transactions on Nuclear Science* 53(6), 3103–3121 (2006)
4. Bashyal, S., Venayagamoorthy, G.K.: Human swarm interaction for radiation source search and localization. In: *Swarm Intelligence Symposium, 2008. SIS 2008*. IEEE. pp. 1–8. IEEE (2008)
5. Berger, M.J., C.J.Z.M., Chang, J.: Estar, pstar, and astar: Computer programs for calculating stopping-power and range tables for electrons, protons, and helium ions (version 1.2.3) [online], <http://physics.nist.gov/Star>
6. Collaboration, T.A.: The atlas experiment at the cern large hadron collider. *Journal of Instrumentation* 3(08), S08003 (2008), <http://stacks.iop.org/1748-0221/3/i=08/a=S08003>
7. Dervan, P., French, R., Hodgson, P., Marin-Reyes, H., Parker, K., Wilson, J., Baca, M.: Upgrade to the birmingham irradiation facility. *Nuclear Instruments and Methods in Physics Research Section A: Accelerators, Spectrometers, Detectors and Associated Equipment* 796, 80–84 (2015)
8. Dervan, P., French, R., Hodgson, P., Marin-Reyes, H., Wilson, J.: The birmingham irradiation facility. *Nuclear Instruments and Methods in Physics Research Section A: Accelerators, Spectrometers, Detectors and Associated Equipment* 730, 101–104 (2013)
9. French, R., Marin-Reyes, H., Kourlitis, E.: Usability study to qualify a dexterous robotic manipulator for high radiation environments. In: *Emerging Technologies and Factory Automation (ETFA), 2016 IEEE 21st International Conference on*. pp. 1–6. IEEE (2016)
10. Jik Lee, H., Kwang Lee, J., Suk Park, B., Sup Yoon, J.: Bridge transported servo manipulator system for remote handling tasks under a radiation environment. *Industrial Robot: An International Journal* 36(2), 165–175 (2009)
11. Kourlitis, E., French, R., Marin-Reyes, H.: Radiation exposure assessment of a robot hand system, chap. 7, pp. 356–365. World Scientific (2016)
12. u. Lee, S., s. Choi, Y., m. Jeong, K., Jung, S.: Development of a tele-operated underwater robotic system for maintaining a light-water type power reactor. In: *2006 SICE-ICASE International Joint Conference*. pp. 3017–3021 (Oct 2006)
13. Leroy, Rancoita: Electromagnetic interaction of charged particles in matter, chap. 2, p. 74. World Scientific (2016)
14. Marin-Reyes, H., French, R., Hodgson, P., Parker, K., Wilson, J., Dervan, P.: Pre-configured XY-Axis cartesian robot system for a new ATLAS scanning facility, chap. 8, pp. 477–483. World Scientific (2014)
15. Nagatani, K., Kiribayashi, S., Okada, Y., Otake, K., Yoshida, K., Tadokoro, S., Nishimura, T., Yoshida, T., Koyanagi, E., Fukushima, M., et al.: Gamma-ray irradiation test of electric components of rescue mobile robot quince. In: *Safety, Security, and Rescue Robotics (SSRR), 2011 IEEE International Symposium on*. pp. 56–60. IEEE (2011)

16. Nancekievill, M., Watson, S., Green, P.R., Lennox, B.: Radiation tolerance of commercial-off-the-shelf components deployed in an underground nuclear decommissioning embedded system. In: 2016 IEEE Radiation Effects Data Workshop (REDW). pp. 1–5 (July 2016)
17. Sharp, R., Decreton, M.: Radiation tolerance of components and materials in nuclear robot applications. *Reliability Engineering & System Safety* 53(3), 291–299 (1996)
18. Weide-Zaage, K., Eichin, P., Chen, C., Zhao, Y., Zhao, L.: Cots - radiation effects approaches and considerations. In: 2017 Pan Pacific Microelectronics Symposium (Pan Pacific). pp. 1–8 (Feb 2017)